

## Coulomb deexcitation of pionic hydrogen within the close-coupling method

V. N. Pomerantsev and V. P. Popov

*Institute of Nuclear Physics, Moscow State University, Moscow, Russia*

(Received 9 November 2005; published 5 April 2006)

The Coulomb deexcitation of the pionic hydrogen atom in collisions with the hydrogen atom has been studied in the quantum mechanical close-coupling approach. The total Coulomb deexcitation cross sections of  $nl \rightarrow n'l'$  transitions and  $l$ -averaged cross sections are calculated for initial states with  $n=3-8$  and at relative energies  $E=0.01-100$  eV. The strong interaction and vacuum polarization shifts of  $ns$  states are taken into account. It is shown that the  $\Delta n > 1$  transitions are very important and make up a substantial fraction of the Coulomb deexcitation cross section (up to  $\sim 47\%$ ).

DOI: [10.1103/PhysRevA.73.040501](https://doi.org/10.1103/PhysRevA.73.040501)

PACS number(s): 36.10.-k

Pionic hydrogen atoms are formed in highly excited states and the evolution of their distributions with quantum numbers and kinetic energy is defined by the competition of both collisional and radiative deexcitation processes during the atomic cascade. Interest in the problem has attracted special attention after the experimental observation of pionic hydrogen atoms with a high kinetic energy up to 200 eV at the instant of the charge exchange reaction  $\pi^-p \rightarrow \pi^0n$  [1-4]. The observed Doppler broadening of the neutron time-of-flight (NTOF) spectra in the experiments is attributed to the Coulomb deexcitation (CD) process, where the energy of the transition is shared between the colliding objects. In order to analyze the above-mentioned and the new experiments [5-8] on the precision spectroscopy of  $K$  x-rays from pionic atoms, the kinetic-energy distribution of pionic hydrogen must be calculated in a realistic cascade model.

The first theoretical study of the CD processes was carried out in the framework of the two-state semiclassical model [9] with some additional approximations (e.g.,  $n \gg 3$ ). Later, the process was considered in a number of papers within the advanced adiabatic [10-12] and the classical-trajectory Monte Carlo [13] approaches. For the low-lying  $n$  states of pionic hydrogen and at low collisional energies the approaches [9,13] cannot be expected to give a reliable description of the CD process. At the same time the rates of the CD process obtained in [10-12] for the  $n \rightarrow n-1$  transitions ( $n=3-5$ ) are more than one order of magnitude smaller than in [9] and are unable to explain the observed kinetic-energy distribution [14] of  $(\pi^-p)$  atoms at the instant of the charge exchange reaction  $\pi^-p \rightarrow \pi^0n$ . Therefore, in the most important region of  $n=3-7$  relevant for kinetics of the atomic cascade the theoretical results are rather undefined and this process is regarded as the least known process of the pionic cascade.

In this paper, we report results for the CD process of  $\pi^-p$  atom in collisions with H obtained in the framework of a fully quantum-mechanical approach. We use the close-coupling (CC) method, in which the scattering processes

$$(\pi^-p)_{nl} + H_{1s} \rightarrow (\pi^-p)_{n'l'} + H_{1s}, \quad (1)$$

such as elastic scattering ( $n'=n, l'=l$ ), Stark transitions ( $n'=n, l' \neq l$ ), and CD ( $n' < n$ ) are described in a unified man-

ner. The energy shifts of the pionic hydrogen  $ns$  states due to the vacuum polarization and strong interaction are taken into account. The method has been recently employed for the study of the CD process in muonic hydrogen [15], where substantially new results in comparison with those known in the literature [9,16] have been obtained. Unless otherwise stated atomic units (a.u.) [ $\hbar=e=m_e m_p / (m_e + m_p) = 1$ ] will be used throughout the paper.

The Hamiltonian of the system  $[(\pi^-p)_{nl} + H_{1s}]$  (after separation of the c.m. motion) is given by

$$H = -\frac{1}{2m} \Delta_{\mathbf{R}} + h_{ex}(\boldsymbol{\rho}) + h_H(\mathbf{r}) + V(\mathbf{r}, \boldsymbol{\rho}, \mathbf{R}), \quad (2)$$

where  $m$  is the reduced mass of the system,  $\mathbf{R}$  is the radius vector between the c.m. of the colliding atoms, and  $\boldsymbol{\rho}$  and  $\mathbf{r}$  are their inner coordinates. The interaction potential  $V(\mathbf{r}, \boldsymbol{\rho}, \mathbf{R})$  is a sum of four Coulomb pair interactions between the projectile atom and the target atom particles.  $h_{ex}(\boldsymbol{\rho})$  and  $h_H(\mathbf{r})$  are the hydrogen-like Hamiltonians of the free exotic and hydrogen atom, whose eigenfunctions together with the angular wave function  $Y_{L\Lambda}(\hat{\mathbf{R}})$  of the relative motion form the basis states  $|1s, nl, L: JM\rangle$ , with the conservation of the total angular momentum ( $JM$ ) and parity  $\pi = (-1)^{l+L}$ . In the present consideration we use the "frozen" electron approximation. This approximation leads to underestimation of the long-range interaction which effects mainly on the elastic and Stark scattering. The influence of the target electron excitation on the CD process is not essential since this process is mainly determined by the short-range part of interaction. The CC approach can be extended in a straightforward manner to include the target electron excitations.

The total wave function of the system is expanded in terms of the basis states as follows

$$\Psi_E^{JM\pi}(\mathbf{r}, \boldsymbol{\rho}, \mathbf{R}) = R^{-1} \sum_{nlL} G_{nlL}^{J\pi}(R) |1s, nl, L: JM\rangle. \quad (3)$$

The expansion (3) leads to the close-coupling second-order differential equations for the radial functions of the relative motion,  $G_{nlL}^{J\pi}(R)$ :

$$\begin{aligned} & \left( \frac{d^2}{dR^2} + k_n^2 - \frac{L(L+1)}{R^2} \right) G_{n'l}^{J\pi}(R) \\ &= 2m \sum_{n'l'L'} W_{n'l'L',n'l}^{J\pi}(R) G_{n'l'L'}^{J\pi}(R). \end{aligned} \quad (4)$$

The channel wave number is defined as  $k_n^2 = 2m(E_{c.m.} + E_{n_0 l_0} - E_{nl})$ , where  $E_{c.m.}$  and  $(n_0 l_0)$  are the energy of the relative motion and the exotic atom quantum numbers in the entrance channel, respectively. The bound energy of the  $\pi^- p$  atom,  $E_{nl} = \varepsilon_{nl} + \Delta\varepsilon_{nl}$ , includes the eigenvalue of  $h_{ex}(\boldsymbol{\rho})$ ,  $\varepsilon_{nl}$ , and the energy shift  $\Delta\varepsilon_{nl} = \Delta\varepsilon_{nl}^{vp} + \Delta\varepsilon_{nl}^{str}$  due to the vacuum polarization and strong interaction. Hereafter, the energy  $E_{c.m.}$  will be referred to  $\varepsilon_{nl \neq 0}$  in the entrance channel (we assume that  $\Delta\varepsilon_{nl \neq 0} = 0$ ).<sup>1</sup>

The matrix elements of the interaction potential

$$W_{n'l'L',n'l}^J(R) = \langle 1s, n'l', L': JM | V | 1s, nl, L: JM \rangle \quad (5)$$

are obtained by averaging it over the electron wave function of the  $1s$  state and then applying the multipole expansion. The integration over  $(\boldsymbol{\rho}, \hat{\mathbf{R}})$  reduces the matrix elements (5) to a multiple finite sum (for more details, see [15]).

At fixed  $E_{c.m.}$  the coupled differential equations (4) for the given  $J$  and  $\pi$  values are solved numerically by the Numerov method with standing-wave boundary conditions involving the real symmetrical  $K$  matrix related to the  $T$  matrix by the equation  $T = 2iK/(I - iK)$ . All exotic atom states with  $n$  values from 1 up to  $n_0$  have been included in the close-coupling calculations. The following cross sections will be discussed: the partial cross section,

$$\sigma_{nl \rightarrow n'l'}^J(E) = \frac{\pi}{k_n^2} \frac{2J+1}{2l+1} \sum_{LL'\pi} |T_{nlL \rightarrow n'l'L'}^{J\pi}|^2, \quad (6)$$

the total cross section of the transition  $nl \rightarrow n'l'$ ,

$$\sigma_{nl \rightarrow n'l'}(E) = \sum_J \sigma_{nl \rightarrow n'l'}^J(E), \quad (7)$$

the total cross section from the  $ns$  state,

$$\sigma_{ns \rightarrow n'}(E) = \sum_{l'} \sigma_{ns \rightarrow n'l'}(E), \quad (8)$$

and the  $l$ -averaged cross section ( $l > 0$ ),

$$\sigma_{nn'}^{l>0}(E) = \frac{1}{n^2 - 1} \sum_{l>0, l'} (2l+1) \sigma_{nl \rightarrow n'l'}(E). \quad (9)$$

We assume that the pionic atom states with  $l \neq 0$  are degenerate and the  $l$ -averaged cross section (9) can be used to illustrate the basic features of the CD process.

The CC calculations of the CD cross sections Eqs. (6)–(9) were carried out for  $(\pi^- p)_{nl} + \text{H}$  collisions for  $n=3-8$  and at

<sup>1</sup>The strong interaction shifts are calculated according to  $\Delta\varepsilon_{ns}^{str} = \Delta\varepsilon_{1s}^{str}/n^3$ , where  $\Delta\varepsilon_{1s}^{str} = -7.11$  eV from [17]. The next values [18] [−3.24 eV (1s), −0.37 eV (2s), and −0.11 eV (3s)] for the vacuum polarization shifts are used in the calculations. For  $n > 3$  we assume  $\Delta\varepsilon_{ns}^{vp} = \Delta\varepsilon_{n-1,s}^{vp} [(n-1)/n]^3$ .

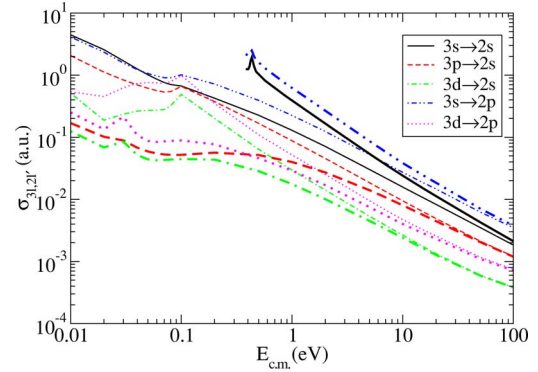


FIG. 1. (Color online) The CD cross sections  $\sigma_{3l,2l'}$  for  $(\pi p)_{3l} + \text{H}$  collisions calculated both with (thick lines) and without (thin lines) taking the  $ns$ -state energy shifts into account.

energy range  $E_{c.m.} = 0.01 - 100$  eV. Summation over the partial waves in Eq. (7) was done up to a value  $J_{max}$  until an accuracy better than 0.1% was reached at all energies. The analysis of the  $J$  dependence of the partial cross sections  $\sigma_{nl \rightarrow n'l'}^J$  shows that most CD cross sections give partial waves with rather low  $J$  values as compared with the elastic scattering and Stark transition processes. Besides, our study shows that a significant underestimation of the CD cross sections (up to one order of magnitude) can be obtained if one neglects the higher-multipole terms in the expansion of the coupling matrix (5). Such a strong effect together with the relatively low  $J$  values involved in the inelastic transitions are related with the fact that the CD process is determined more by the more short-range interaction than the elastic and Stark scattering.

In order to illustrate the influence of the  $ns$  state energy shifts on the CD cross sections, the calculations were performed both with and without taking energy shifts into account. The effect is the most pronounced for the low-lying states and some of the results for  $n=3,4$  are shown in Figs. 1 and 2 and presented in Table I.

The CD cross sections for a number of transitions  $3l$

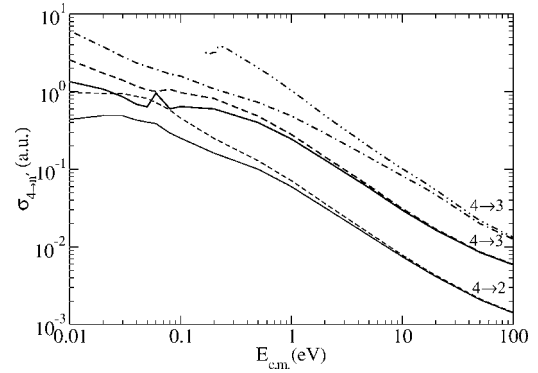


FIG. 2. The  $l$ -averaged CD cross sections  $\sigma_{4,3}^{l>0}$  (thick lines) and  $\sigma_{4,2}^{l>0}$  (thin lines) for  $(\pi p)_{4l} + \text{H}$  collisions calculated with (solid lines) and without (dashed lines) taking the  $s$ -state energy shifts into account. The CD cross sections  $\sigma_{4 \rightarrow 3}^{J=0}$  calculated both with (double-dot-dashed line) and without (dot-dashed line) taking  $s$ -state energy shifts into account are also shown.

TABLE I. The CD cross sections  $\sigma_{n,n'}^{l>0}$  for  $(\pi p)_n + \text{H}$  collisions (in a.u.) calculated in the quantum-mechanical CC approach.

$E_{\text{c.m.}}$ (eV)	0.01	0.02	0.03	0.05	0.08	0.1	0.2	0.5	1.0	2.0	5.0	7.0	10	20	50	100
$\sigma_{32}$	0.409	0.231	0.289	0.145	0.138	0.143	0.139	0.102	0.072	0.046	0.022	0.017	0.012	0.007	0.003	0.002
$\sigma_{32}^{(\Delta\epsilon=0)}$	2.261	1.315	1.293	1.303	1.275	1.711	0.770	0.293	0.148	0.075	0.030	0.021	0.015	0.008	0.004	0.002
$\sigma_{43}$	1.342	1.076	0.858	0.638	0.958	0.642	0.599	0.399	0.245	0.132	0.058	0.042	0.030	0.017	0.009	0.006
$\sigma_{43}^{(\Delta\epsilon=0)}$	2.558	1.728	1.402	1.052	1.004	0.969	0.814	0.483	0.280	0.145	0.062	0.044	0.031	0.017	0.009	0.006
$\sigma_{42}$	0.438	0.491	0.489	0.404	0.387	0.252	0.161	0.100	0.060	0.032	0.014	0.010	0.007	0.004	0.002	0.001
$\sigma_{42}^{(\Delta\epsilon=0)}$	0.977	0.946	0.942	0.817	0.721	0.456	0.250	0.129	0.071	0.036	0.015	0.011	0.008	0.004	0.002	0.001
$\sigma_{54}$	3.497	2.672	1.750	1.201	1.055	0.769	0.531	0.314	0.202	0.125	0.060	0.044	0.033	0.020	0.013	0.012
$\sigma_{53}$	0.929	1.118	0.677	0.417	0.355	0.251	0.177	0.091	0.050	0.025	0.010	0.007	0.005	0.003	0.002	0.001
$\sigma_{52}$	0.188	0.292	0.199	0.122	0.103	0.074	0.069	0.040	0.022	0.011	0.005	0.004	0.003	0.001	0.001	0.001
$\sigma_{65}$	3.644	2.510	2.423	1.544	1.121	1.012	0.636	0.298	0.169	0.098	0.041	0.031	0.024	0.016	0.015	0.020
$\sigma_{64}$	1.446	1.309	1.232	0.903	0.683	0.603	0.377	0.217	0.129	0.068	0.028	0.021	0.015	0.009	0.005	0.004
$\sigma_{63}$	0.436	0.349	0.265	0.171	0.115	0.098	0.065	0.032	0.017	0.008	0.003	0.002	0.002	0.001	0.001	0.001
$\sigma_{76}$	5.647	4.321	3.202	2.636	2.157	1.747	1.247	0.590	0.346	0.190	0.082	0.061	0.045	0.027	0.023	0.038
$\sigma_{75}$	1.545	1.272	0.793	0.696	0.762	0.527	0.319	0.150	0.095	0.053	0.023	0.018	0.014	0.009	0.007	0.008
$\sigma_{74}$	0.300	0.280	0.154	0.156	0.162	0.114	0.069	0.037	0.019	0.010	0.004	0.003	0.002	0.002	0.001	0.002
$\sigma_{87}$	7.480	4.541	4.095	3.379	3.217	2.379	1.757	1.003	0.662	0.371	0.159	0.118	0.086	0.051	0.042	0.077
$\sigma_{86}$	1.340	0.925	0.822	0.719	0.624	0.485	0.378	0.190	0.130	0.072	0.031	0.023	0.017	0.011	0.010	0.016
$\sigma_{85}$	0.571	0.340	0.315	0.362	0.234	0.222	0.170	0.078	0.044	0.023	0.010	0.008	0.006	0.004	0.003	0.004

$\rightarrow 2l'$  with or without the energy shifts of the  $ns$  states are shown in Fig. 1. In case  $\Delta\epsilon_{ns} \neq 0$  the energy dependence of the cross sections changes crucially. The cross sections corresponding to the  $3p(3d) \rightarrow 2s, 2p$  transitions at energies above and below the threshold of the Stark transitions  $3s \rightarrow 3p, 3d$  are strongly suppressed. The effect is more clearly observed at energies in the vicinity of 0.1 eV (the suppression is more than or about one order of the magnitude). At  $E_{\text{c.m.}} \gg |\Delta\epsilon_{ns}|$  the differences between the corresponding pair of the curves (see Fig. 1) are negligible at  $E_{\text{c.m.}} \geq 15$  eV for  $n=3$  and at  $E_{\text{c.m.}} \geq 1$  eV for  $n=4$ . On the contrary, the transitions  $3s \rightarrow 2s, 2p$  are enhanced at the threshold by a factor about 3–4. The main reason for such behavior of the CD cross section is related to the inelastic nature of the Stark transitions due to the  $s$ -state shift.

The similar regularities are also observed in the

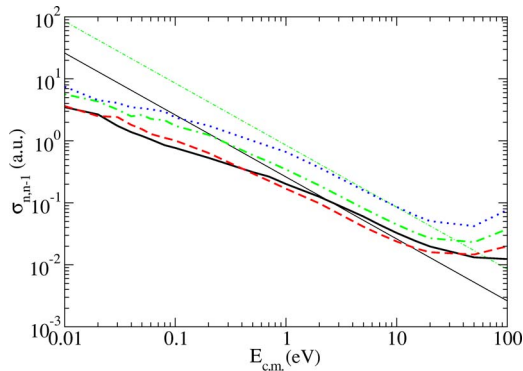


FIG. 3. (Color online) The  $l$ -averaged CD cross sections  $\sigma_{n,n-1}^{l>0}$  for  $(\pi p)_n + \text{H}$  collisions with  $n=5$  (solid line), 6 (dashed), 7 (dot-dashed), and 8 (dotted). The results of the parametrization [13] for  $n=5$  and 7 are shown (thin lines).

$l$ -averaged CD cross sections. In Fig. 2 (see also Table I) the  $l$ -averaged CD cross sections for the  $4 \rightarrow 3$  and  $4 \rightarrow 2$  transitions and total cross sections from the  $4s$  state are presented. One can see that the maximal suppression due to the energy shift of the  $4s$  state is weaker and less than or about two times at very low energy for both  $4 \rightarrow 3$  and  $4 \rightarrow 2$  transitions, while at  $E_{\text{c.m.}} > 1$  eV it does not exceed 15%. The important observation follows from Fig. 2 and Table I. The CD cross sections for the  $\Delta n \geq 2$  transitions are strongly enhanced as compared with the previous studies and their relative contribution to the CD process varies from 20% up to 47% for  $n \geq 4$ .

CD cross-section behavior like  $\sim n^\gamma/E$  based on the results of [9] is commonly used in cascade calculations. In order to illustrate our results the  $l$ -averaged CD cross sections ( $l > 0$ ) for  $n=5-8$  and  $\Delta n=1$  are shown in Fig. 3. The straight lines show the results of the parametrization [13], based on the simple mass scaling of the CD cross sections

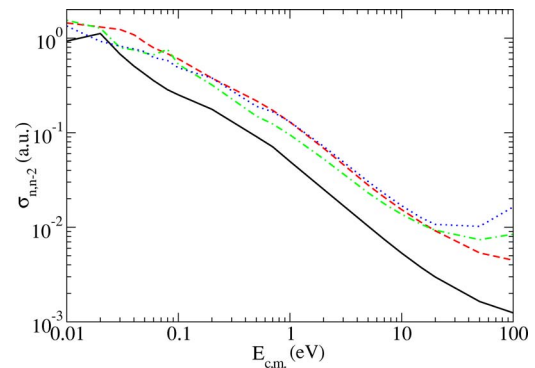


FIG. 4. (Color online) The same as in Fig. 3 but for transitions  $n \rightarrow n-2$ .

for muonic hydrogen [9]. As is seen from Fig. 3, the energy dependence of the CD cross sections only in the region  $1 \leq E \leq 10$  eV, as a whole, is in qualitative agreement with  $1/E$  dependence. But at the energies beyond this interval the energy dependence of the present cross section is quite different. In particular, at  $E \leq 1$  eV our results show close to  $E^{-1/2}$  behavior of the CD cross sections in accordance with the Wigner threshold law [19] and in disagreement with the  $1/E$  dependence obtained in the semiclassical model [9] and advanced adiabatic approach [10–12].

Concerning the power  $n$  dependence nearly to  $n^\gamma$  with  $\gamma > 2$ , the present consideration does not confirm that the CD cross sections have such a scale factor depending on  $n$  (see Fig. 3 and Table I). Moreover, the nonmonotonic behavior of  $\sigma_n^{CD}$  as a function of  $n$  is revealed for all  $n$  under consideration.

The present calculations show that  $\Delta n=1$  transitions dominate. According to our CC calculations (see Fig. 4 and Table I), the  $\Delta n > 1$  transitions make up a substantial fraction (20–47%) of the total CD cross sections for  $n \geq 4$  at all the energies under consideration. It is worthwhile noting that there is no simple power  $n$  dependence of the CD cross sections for the  $\Delta n > 1$  transitions either. The regular  $n$  dependence appears at relative energies more than or about 50–70 eV (Fig 5).

In summary, the CD process in pionic hydrogen has been studied in the fully quantum-mechanical CC approach, involving simultaneously the elastic and Stark processes. The obtained results reveal the additional knowledge about the

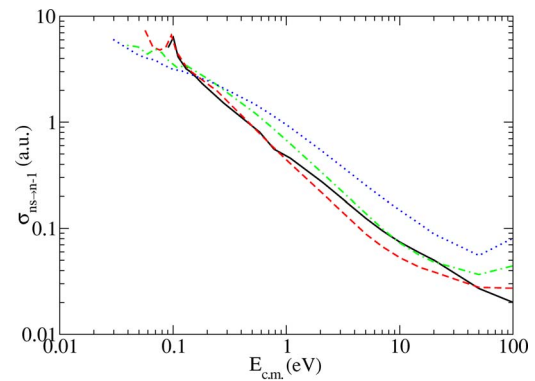


FIG. 5. (Color online) The CD cross sections from  $s$  states  $\sigma_{ns \rightarrow n-1}$  for  $n=5-8$ . The notations of the curves are the same as in Figs. 3 and 4.

CD process and are very important for the reliable analysis of the  $K$  x-ray yields and NTOF spectra.<sup>2</sup>

We are grateful to Professor G. Korenman for fruitful discussions. This work was partially supported by Russian Foundation for Basic Research Grant No. 06-02-17156.

<sup>2</sup>We thank T. Jensen for the preliminary results of the analysis with the present CD cross sections of the NTOF spectra [3]. Our results explain the high energy component around 105 eV due to the  $5 \rightarrow 3$  transition and lead to a very good agreement with the experimental weight of the  $3 \rightarrow 2$  component at 209 eV.

- 
- [1] J. F. Crawford, M. Daum, R. Frosch, B. Jost, P.-R. Kettle, R. M. Marshall, B. K. Wright, and K. O. H. Ziock, *Phys. Rev. D* **43**, 46 (1991).
- [2] E. C. Aschenauer *et al.*, *Phys. Rev. A* **51**, 1965 (1995).
- [3] A. Badertscher *et al.*, *Phys. Lett. B* **392**, 278 (1997).
- [4] J. Schottmüller *et al.*, *Hyperfine Interact.* **119**, 95 (1999).
- [5] L. M. Simons, *Hyperfine Interact.* **119**, 281 (1999).
- [6] D. F. Anagnostopoulos *et al.*, *Hyperfine Interact.* **138**, 131 (2001); *Nucl. Phys. A* **721**, c849 (2003).
- [7] D. Chatellard *et al.*, *Nucl. Phys. A* **625**, 855 (1997).
- [8] D. Sigg *et al.*, *Phys. Rev. Lett.* **75**, 3245 (1995); *Nucl. Phys. A* **609**, 269 (1996).
- [9] L. Bracci and G. Fiorentini, *Nuovo Cimento Soc. Ital. Fis., A* **43**, 9 (1978).
- [10] A. V. Kravtsov and A. I. Mikhailov, *JETP* **80**, 822 (1995); *Phys. Rev. A* **58**, 4426 (1998).
- [11] L. I. Ponomarev and E. A. Solov'ev, *JETP Lett.* **64**, 135 (1996).
- [12] A. V. Kravtsov, A. I. Mikhailov, L. I. Ponomarev, and E. A. Solovyev, *Hyperfine Interact.* **138**, 99 (2001).
- [13] T. S. Jensen and V. E. Markushin, *Eur. Phys. J. D* **21**, 261 (2002); **21**, 271 (2002).
- [14] A. Badertscher *et al.*, *Europhys. Lett.* **54**, 313 (2001).
- [15] G. Ya. Korenman, V. N. Pomerantsev, and V. P. Popov, *JETP Lett.* **81**, 543 (2005); e-print nucl-th/0501036.
- [16] L. I. Ponomarev and E. A. Solovyov, *Phys. At. Nucl.* **65**, 1575 (2002).
- [17] H.-Ch. Schröder *et al.*, *Eur. Phys. J. C* **21**, 473 (2001).
- [18] S. Jonsell, J. Wallenius, and P. Froelich, *Phys. Rev. A* **59**, 3440 (1999).
- [19] E. P. Wigner, *Phys. Rev.* **73**, 1002 (1948).